

Received July 12, 2020, accepted August 6, 2020, date of publication August 14, 2020, date of current version August 26, 2020.

Digital Object Identifier 10.1109/ACCESS.2020.3016770

Coexistence Analysis of Multiple Asynchronous IEEE 802.15.4 TSCH-Based Networks

FARZAD VEISI¹, MAJID NABI^{1,2}, (Member, IEEE), AND HOSSEIN SAIDI¹

¹Department of Electrical and Computer Engineering, Isfahan University of Technology, Isfahan 84156-83111, Iran

²Department of Electrical Engineering, Eindhoven University of Technology, 5600 Eindhoven, The Netherlands

Corresponding author: Majid Nabi (m.nabi@tue.nl)

This work was supported by the Electronic Component Systems for European Leadership (ECSEL) Joint Undertaking through the SCOTT European Project (www.scott-project.eu) under Grant agreement 737422.

ABSTRACT Low-power Wireless Sensor Networks (WSNs) play a key role in realization of the Internet-of-Things (IoT). Among others, Time Slotted Channel Hopping (TSCH) is a Medium Access Control (MAC) operational mode of the IEEE 802.15.4 standard developed for communications in short range IoT networks. TSCH provides high level reliability and predictability by its channel hopping mechanism and time division channel access nature. In many applications, a number of TSCH networks may coexist in the same neighborhood. Several vehicles close to one another, each including a TSCH network for its in-vehicle communications, serve as an example. Since such networks are running independent of one another, they are not expected to be synchronized in time, and they are not scheduled to operate in exclusive frequency channels. This may lead to inter-TSCH interferences deteriorating the reliability of the networks, which is an important requirement for many IoT applications. This paper analyzes the impact of multiple asynchronous TSCH networks on one another. An analytical model is developed that estimates the chance of such interferences, and the expectation of the number of affected TSCH channels when a number of them are in the vicinity of one another. The developed model is verified using extensive simulations and real-world experiments. Also, a scalable and fast multi-TSCH coexistence simulator is developed that is used to get insight about coexistence behaviors of any number of TSCH networks with various configurations.

INDEX TERMS Internet-of-Things, wireless sensor networks, coexistence, IEEE 802.15.4, TSCH.

I. INTRODUCTION

As a major building block of the Internet-of-Things (IoT), a number of low-power wireless devices communicate with one another to sense and deliver sensor data, forming a Wireless Sensor Network (WSN). The IEEE 802.15.4 [1] standard is one of the most widely used communication technologies in WSNs, providing the physical and Medium Access Control (MAC) layers' specifications. This standard operates in the unlicensed 2.4 GHz ISM frequency band and is basically designed for low-power, low-cost, and low data rate applications. Time Slotted Channel Hopping (TSCH) is one of the MAC operational modes of this standard, which is mainly developed for industrial applications in which higher communication reliability and predictability is required. The main features of this mode are the use of Time Division Multiple Access (TDMA) together with a frequency channel hopping. The TDMA mechanism of TSCH makes the communications more efficient and predictable by avoiding

intra-TSCH collisions. On the other hand, channel hopping reduces the impact of multi-path fading, and external interference from coexisting wireless technologies (e.g., Wi-Fi and Bluetooth) operating in the same frequency band.

In many IoT applications, a number of independent TSCH networks may coexist in a neighborhood. A motivating example is wireless in-vehicle networks. Since TSCH is designed for reliable industrial applications, it is considered as a promising option for communication of various devices (sensors, actuators, and microprocessors) within a vehicle [2]. However, there are many cases (e.g., behind traffic lights or in the parking lots) in which several vehicles are very close to one another in a period of time. Considering typically low transmission power used in such low-power networks, we can expect around up to ten vehicles to be in the communication range of one another in these scenarios. As another example, TSCH may be used as the communication technology for wireless networking of (bio)sensors installed on/in a patient's body [3], forming a Wireless Body Area Network (WBAN). Now consider that such patients in a hospital or care center may get close, and thus their TSCH networks start interfering

The associate editor coordinating the review of this manuscript and approving it for publication was Hongwei Du.

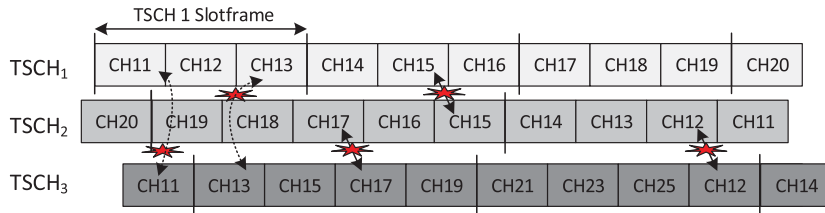


FIGURE 1. Slotframes of three coexisting independent TSCH networks as an illustrative example.

one another. In a gathering event, it may happen that tens of such independent TSCH networks coexist for some duration in time.

Although, within a TSCH network, the nodes are synchronized, and timeslots are exclusively allocated to different transmitting nodes to avoid intra-TSCH collisions, different coexisting TSCH networks may collide with one another. This is because different TSCH networks are organized independently meaning that their timeslots are not aligned with one another, and they are not scheduled exclusively across different TSCH networks. Such inter-TSCH interferences may lead to long term disconnections, and eventually degradation of the reliability and real-time performance of the networks. On the other hand, it is possible that multiple TSCH networks coexist without interfering one another. This coexistence without interference may happen due to the fact that packet transmissions in various coexisting TSCH networks may not be overlapping in time or frequency. Even when two TSCH networks happen to use the same frequency channels, they may still have no interference because of specific timing of their packet transmissions within their timeslots.

This paper aims at modeling and analysis of interference between multiple asynchronous TSCH networks. It analyzes the chances with which different TSCH networks use the same channel according to their exact channel hopping sequences. Fig. 1 illustrates the situation for overlapping channel usage by three TSCH networks with different lengths of slotframes. The first network (*TSCH*₁) uses the same channel as the one used by *TSCH*₃ in two timeslots (its first and third timeslots). Also, *TSCH*₁ uses the same channel as the one used by *TSCH*₂ in its fifth timeslot. When some TSCH networks operate in the same channel, they may still communicate without interfering one another depending on the time deviation between the boundaries of their timeslots. For such cases, we develop a model using the convolution of the timeslots' structures to acquire the chance of interference-free communication of the coexisting co-channel TSCH networks, taking into account the transmission timing of data and the optional acknowledge (Ack) packets within the timeslot. The time-domain analysis of co-channel TSCH networks is verified and confirmed by Cooja simulations as well as real-world experiments using wireless sensor devices.

After analysis of the chance of time-overlap between co-channel TSCH communications, the chance of being co-channel is analyzed when a number of channel hopping

TSCH networks are in the range of one another. Such kinds of time and frequency channel inter-TSCH interference breakdown can be used as the basis for designing proper run-time adaptive mechanisms to avoid trapping in the worst-case situations which may lead to application failure. Since the length of data and Ack packets, and channel hopping sequences in each TSCH network and their relative time deviations influence the probability of inter-TSCH interferences, there can be extremely high number of coexistence scenarios that may happen when a number of TSCH networks are in the interference range of one another. To get a true insight of the worst/best/average case scenarios, a scalable multi-TSCH coexistence simulator is developed, which is used to perform Monte Carlo simulations to get statistical behavior of the coexistence of these networks.

The rest of the paper is organized as follows. Section II presents the required background on the TSCH technology standard. Section III reviews the related work in this domain. Section IV analyzes the chance of overlap in time provided that two TSCH networks are overlapping in frequency. It then follows by presenting the experimental verification of the analysis. Section V investigates the chance of overlap in a frequency channel when several TSCH networks coexist. The developed TSCH coexistence simulation framework is presented in Section VI, and the simulation results for various number of coexisting TSCH networks are discussed. Section VII concludes.

II. TSCH BACKGROUND

TSCH is an operational mode of the IEEE 802.15.4 standard which is developed for industrial applications. The physical layer of this standard is the same as the one used in the base IEEE 802.15.4 physical layer. Thus the same IEEE 802.15.4-compliant radio transceiver chip can be used for TSCH implementation. The 2.4 GHz frequency band using the O-QPSK + DSSS modulation scheme is the most widely used physical layer for this standard, providing a bit rate of 250 kbps. There are 16 channels (channel 11 to 26) available in this frequency band, each with 2 MHz bandwidth and channel spacing of 5 MHz.

The main features of TSCH are the TDMA-based medium access layer, and channel hopping. The TDMA mechanism provides the possibility to use a collision-free schedule for accessing the shared medium, which leads to efficient channel usage and more reliability and predictability of the network. In TSCH, time is divided into equal length timeslots.

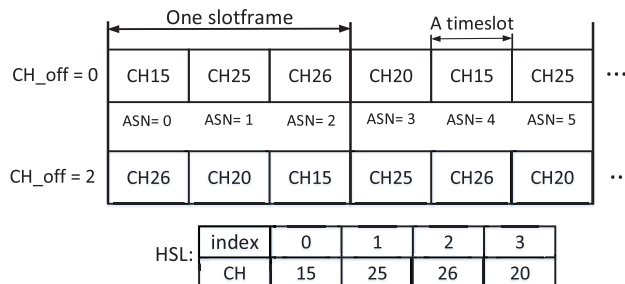


FIGURE 2. The structure of TSCH slotframes with two parallel slotframes.

Each timeslot is long enough for the exchange of a data packet and its (optional) acknowledgment between a pair of nodes. A number of timeslots is called a slotframe which repeats over time. Fig. 2 illustrates the structure of a slotframe containing three timeslots. Wireless nodes align the boundaries of their timeslots using a synchronization mechanism specified by the standard. Moreover, there is a guard time at the beginning of each timeslot to compensate for small misalignments caused by clock drifts. A timeslot may be dedicated to a node in a neighborhood for its collision-free transmission, or it may be shared between nodes to use a special CSMA/CA mechanism for accessing the channel. The TSCH standard does not provide any scheduling mechanism for assigning timeslots for packet transmissions by nodes in the network; this task is left for the upper layers in the protocol stack.

Besides the TDMA mechanism, TSCH implements a channel hopping technique aiming at reducing the impact of multi-path fading and interference. In the 2.4 GHz frequency band, nodes jump to different frequency channels from the 16 available channels in this band. Thus, nodes do not stay in a single channel for their communications. The used channel (CH) in each timeslot is obtained from Eqn. 1.

$$CH = HSL [(ASN + CH_Off)\% |HSL|] \quad (1)$$

The Hopping Sequence List (HSL) is an especially ordered subset of the sixteen frequency channels in the 2.4 GHz ISM frequency band, and $|HSL|$ denotes the number of channels in this list. Absolute Sequence Number (ASN) is a global variable synchronized in the whole TSCH network, which counts the timeslots. TSCH provides the possibility of parallel communication in the network by using different channel offset values (CH_Off). Given the number of available channels, it is possible to create up to sixteen parallel transmissions in a timeslot. Fig. 2 illustrates the channel hopping mechanism in a network using two channel offsets.

III. RELATED WORK

Since there are a number of wireless technology standards operating in the shared 2.4GHz ISM band, there have been quite some efforts in the community to analyze the coexistence of such technologies to understand and anticipate the impact of cross-technology interference on the performance of the coexisting networks. The work presented in [4] investigates the coexistence between IEEE 802.15.4 and

IEEE 802.11b by performing extensive experiments with different configurations. The objective is to acquire insight about coexistence of such networks and optimize their configurations in real-world circumstances. Reference [5] presents a coexistence model for IEEE 802.15.4 and IEEE 802.11b/g, focusing on power and timing aspects. Reference [6] analyzes the coexistence between the IEEE 802.15.4, Bluetooth Low Energy (BLE) [7], and WiFi, from the physical layer perspective assuming that all operate in the same frequency at a given time of transmission. Also, [8] investigates the coexistence between the IEEE 802.11(g and b) and IEEE 802.15.4 networks by analyzing the impact of parameters such as transmission power and traffic scheduling. More specifically on coexistence of TSCH networks with other technologies, [9] investigates the coexistence of WiFi and TSCH in a controlled aircraft cabin through carrying out several real-world experiments in environments with or without interferences. Mainly, this work tries to highlight the importance and effectiveness of frequency hopping against the interference.

Besides coexistence analysis and study, some have tried to develop solutions to alleviate the negative impact of the cross-technology interferences. Reference [10] proposes a coexistence solution to provide a reliable communication for a ZigBee network under heavy WiFi traffic by reserving a frequency channel for ZigBee. Reference [11] proposes an agile algorithm for IEEE 802.15.4 by which it adaptively detects WiFi interferences and dynamically changes the frequency channel. Reference [12] uses some kind of signaling between IEEE 802.15.4 and WiFi to synchronize them, and exclusively share the channel by communicating in their dedicated time frames. Reference [13] proposes a mechanism for coexistence between TSCH and WiFi, by which WiFi sends its packets at idle times of the TSCH networks allowing TSCH to have better performance. In this work, it is supposed that the TSCH network occupies only a tiny portion of time for sending its packets and has a precise synchronization. In [14], the authors present a cooperative coexistence solution for TSCH and BLE in which a scheduling matrix is used by a coordinator node to predict the upfront resource usage (time and frequency) by each network. This is then used to recommend proper channels for each network to avoid interference.

The aforementioned literature focuses on cross-technology interference; none of them addresses the coexisting of multiple independent networks of the same type. The work in [15] presents an analytic model to investigate the performance of uncoordinated coexisting IEEE 802.15.4 networks to support machine-to-machine applications. However, a network running the base IEEE 802.15.4 operates in a single frequency channel and uses a contention-based MAC layer based on CSMA/CA. This is quite different than the TSCH mode in which channel hopping with a TDMA-based collision-free MAC mechanism is used within each network. The inter-TSCH interference in scenarios in which multiple independent TSCH networks coexist is the target of our work.

The work presented in [16] investigates the coexistence of independently administrated TSCH networks using a set of network simulations in Cooja for different values of the clock drift. The impact of clock drift is studied from simulation results. Also, it is investigated how increasing the number of channels in the HSL of the involved TSCH networks can improve the coexistence. However, the tested scenarios in this work are samples of many scenarios that can happen when several networks get very close. In fact, network simulators such as Cooja have speed limitations to be used for performing sufficiently high number of setups to get an overall view of consistence behavior. Moreover, the scale of simulation in terms of the number of networks is limited. These are actually the main reasons that we developed a scalable multi-TSCH coexistence simulator, which allows us to perform Monte Carlo simulations. This gives us a comprehensive insight of the distribution of the coexistence scenarios that can happen.

The only other work that focuses on inter-TSCH interference is [17]. In this work, it is supposed that the timing of different TSCH networks may deviate from one another because of the clock drift between their oscillators. Then, the impact of clock drift on collisions is modeled. However, it assumes that all TSCH networks use a same slotframe length, while in real-world applications, different TSCH networks are presumably independent of one another and may use different slotframe lengths. On the other hand, both [16] and [17] assume that nodes send or receive packets from the beginning to the end of a timeslot, ignoring the details of timeslots' structure in TSCH. It means that if any part of the timeslots overlaps, they consider it as a collision. Our detailed analysis and modeling using the convolution of the timeslots' structures supported by experimental and simulation results show that the chance of interference-free communication of coexisting co-channel TSCH networks can be really high, and thus cannot be simply ignored.

This paper aims at analyzing the coexistence of multiple independent (thus asynchronous) TSCH networks taking into account the details of the timeslots' structure defined by the technology standard, and considering that different TSCH networks may have different settings (e.g., HSL, timeslot length, data and Ack packet length, etc.). Overlaps in both time and frequency channels are modeled and verified by real experiments and Cooja simulations. Finally, a scalable multi-TSCH coexistence simulator is developed that is able to simulate the coexistence of any number of TSCH networks in terms of transmission time and used frequency channel. The extensive simulations using the developed simulator give important insights about various scenarios that may happen when different number of TSCH networks coexist with one another, revealing the worst and best cases extremes.

IV. ANALYSIS OF CO-CHANNEL TSCH NETWORKS

In this section, we first investigate the TSCH timeslot structure in detail and then analyze the case in which two TSCH networks transmit in the same frequency channel. The end goal of such analysis is to find out the possibility

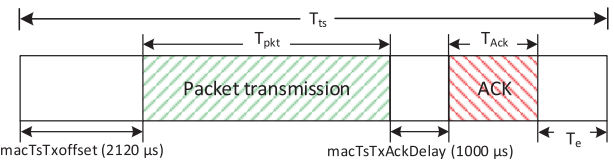


FIGURE 3. The structure of a TSCH timeslot.

of successful packet delivery while two independent TSCH networks use the same channel. Then the results of the experimental verification of the analysis are presented.

A. TSCH TIMESLOT STRUCTURE

Timeslot is the smallest time division in a TSCH network. Fig. 3 shows the structure of a TSCH timeslot together with the default value of some timing parameters. T_{ts} is the length of the timeslot whose default value in the standard is 10 ms. At the beginning of each transmission timeslot, there is a guard time ($macTsTxoffset$) after which the transmission starts by the sender node, to compensate small clock drifts between the sender and receiver(s). The number of bytes in a packet (L_{pkt}) is not fixed and can be up to 133 bytes in the physical layer. Thus the packet transmission duration will be $T_{pkt} = \frac{L_{pkt} \times 8}{250(kbps)}$; it is 4.256 ms for the maximum packet size allowed in the standard. After transmission of a data packet, an optional Ack packet may be transmitted by the receiver after $macTsTxAckDelay$ time; its default value is 1000 μs . T_{Ack} is the air time of the Ack packet which is calculated according to the length of the Ack packet (L_{Ack}). There are two types of Ack packet specified in the standard (i.e., Imm-Ack and Enh-Ack) with different lengths. Depending on the type of the Ack packet, T_{Ack} can be up to 2400 μs .

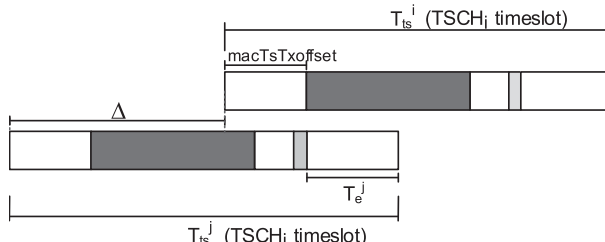
Taking into account the aforementioned time durations from the beginning of a timeslot, there may be some time left at the end before the next timeslot starts. The length of the remaining time (T_e) at the end of the timeslot is given by Eqn. 2.

$$T_e = T_{ts} - (macTsTxoffset + T_{pkt} + macTsTxAckDelay + T_{Ack}) \quad (2)$$

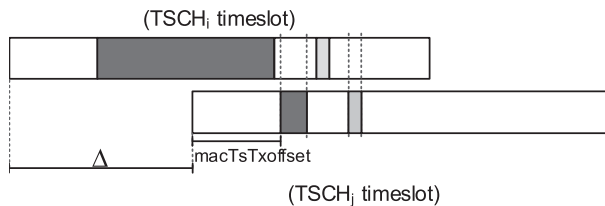
B. TIME OVERLAP ANALYSIS

To investigate the impact of coexisting TSCH networks on one another, we need to analyze their behaviors in both time and frequency domains. If two or more TSCH networks work in different frequency channels in a timeslot, they do not interfere one another. The possibility of such cases are analyzed in the next section. In this section, we start with time analysis of TSCH networks that happen to operate in the same channel in a timeslot or parts of it. Depending on the length of timeslots, packet sizes, and Ack transmission time, it is possible that two TSCH networks have successful packet transmission and Ack reception in a timeslot while they overlap in frequency channel.

To analyze the scenario, assume that two TSCH networks ($TSCH_i$ and $TSCH_j$) are in the communication range of one another. Fig. 4(a) illustrates an example of interference-free



(a) One transmission is completed before the other one starts due to the long enough time deviation (Δ).



(b) The packet and Ack transmissions in two networks are interleaved during a timeslot.

FIGURE 4. Scenarios for successful transmission of co-channel TSCH networks.

co-channel scenario. Since the two TSCH networks are independent of one another, they are not synchronized and there is a Δ time deviation between the start of their timeslots. Taking the start of timeslot in one of the two networks (say $TSCH_i$) as our time reference, Δ can be any value in the range of $-T_{ts}^j \leq \Delta \leq T_{ts}^i$. Communications in both networks depicted in Fig. 4(a) are successful because there is no overlap of transmission durations of the two networks; the packet transmission in $TSCH_j$ is done and acknowledged before the transmission in $TSCH_i$ gets started. Such situation happens whenever Δ value lies in the ranges of $[-T_{ts}^j, macTsTxoffset + T_e - T_{ts}^i]$ or $[T_{ts}^i - (macTsTxoffset + T_e), T_{ts}^i]$, since there will remain enough time either at the beginning or the end of the timeslots for interference-free communication.

The above mentioned scenario is not the only possible interference-free scenario for two co-channel TSCH networks; several other cases can end up with interference-free communications in both networks. As an example, Fig. 4(b) illustrates a case in which the value of Δ is such that the packet and Ack transmission of the two networks nicely interleave with one another. This has happened partially because of very short packet in $TSCH_j$, which is common in many sensor network applications.

To capture all such cases and compute the chance of collision-free communications of two co-channel TSCH networks, we use the convolution of the two timeslots' structures over all possible values of the time deviation Δ . The convolution operation provides a cross-correlation function between the structure of the timeslots in the two networks. Thus, the convolution result indicates the time durations in which the data or Ack packet transmission in the two networks overlap. Since the convolution operation slides the two input functions over one another in the specified range, it examines all possible time deviations between

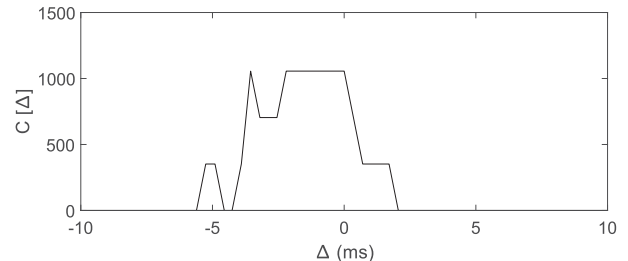


FIGURE 5. Convolution of two timeslots (overlap ratio) in the Ack-enabled mode (T_{ts} for both networks is 10 ms).

the networks. Suppose the Γ_i and Γ_j are two vectors of boolean values (zero or one) that represent signal transmission in $TSCH_i$ and $TSCH_j$, respectively. These vectors are made with a resolution δ ; their lengths are $|\Gamma_i| = \frac{T_{ts}^i}{\delta}$ and $|\Gamma_j| = \frac{T_{ts}^j}{\delta}$. For instance, $\Gamma_i[n] = 1$ means that a signal is being transmitted at time $n \times \delta$ from the beginning of timeslot of $TSCH_i$. Eqn. 3 gives the convolution of the two timeslots. $C[n]$ in actually the *overlap ratio* of the active parts of the two timeslots in time.

$$C[n] = \Gamma_i[n] * \Gamma_j \left[\frac{T_{ts}^j}{\delta} - n \right] \Big|_{0 \leq n \leq \frac{T_{ts}^j + T_{ts}^i}{\delta}} \\ = \sum_{\tau=-T_{ts}^j/\delta}^{T_{ts}^i/\delta} \Gamma_i[\tau] \times \Gamma_j \left[\frac{T_{ts}^j}{\delta} - n - \tau \right] \Big|_{n=\frac{T_{ts}^j + \Delta}{\delta}} \quad (3)$$

The discrete convolution function flips the second vector, which is not what we intend here. That is why the timeslot structure vector Γ_i in Eqn. 3 is flipped by using the index of $\frac{T_{ts}^j}{\delta} - n$. Fig. 5 shows the output of the convolution function (overlap ratio) for an example scenario in which both networks use timeslots with equal length of 10ms with $L_{pkt}^i = 22$ bytes, $L_{Ack}^i = 11$ bytes, $L_{pkt}^j = 133$ bytes, $L_{Ack}^j = 11$ bytes, and resolution of $\delta = 1\mu s$. Note that, in this figure, the convolved vector $C[\Delta]$ is plotted instead of $C[n]$ (i.e., $n = \frac{T_{ts}^j + \Delta}{\delta}$) to directly show the impact of Δ on the convolution output for the full range of Δ from $-T_{ts}^j = -10ms$ to $T_{ts}^i = 10ms$.

To calculate the chance of collision-free coexistence of two networks when they happen to operate in a single frequency channel, we need to measure the total cases in which Δ is such that the overlap ration has a zero value (no concurrent transmissions). From our perspective, Δ has a uniformly random value in its range since the coexisting networks are assumed to be independent and asynchronous. Then, the fraction of the range between $\Delta = -T_{ts}^j$ and $\Delta = T_{ts}^i$ in which $C[\Delta]$ is zero gives the probability with which two independent co-channel TSCH networks do not interfere one another (\bar{P}_c). Eqn. 4 gives this probability,

$$\bar{P}_c = \frac{\delta \times \sum_{n=0}^{(T_{ts}^i + T_{ts}^j)/\delta} F(C[n])}{T_{ts}^i + T_{ts}^j} = \frac{\delta \times \sum_{\Delta=-T_{ts}^j}^{T_{ts}^i} F(C[\Delta])}{T_{ts}^i + T_{ts}^j}, \quad (4)$$

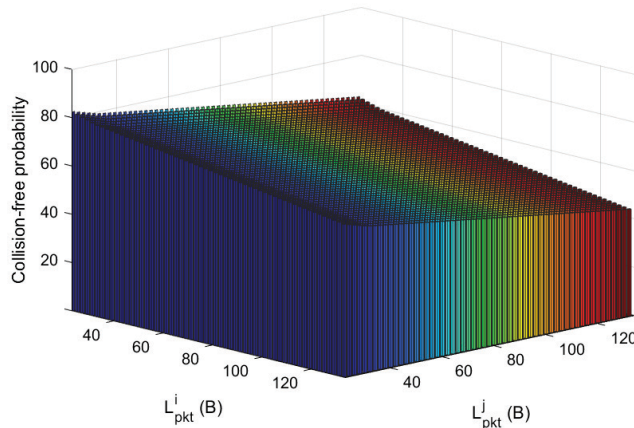


FIGURE 6. Visualization of the chance of interference-free coexistence of two co-channel TSCH networks in the Ack-enabled mode for different packet lengths (both network use timeslots of 10ms).

where $F(x)$ is a function that gives output 1 when its argument $x = 0$; otherwise it gives zero. It is clear that at the end the chance of collision-free communication in two networks depends on parameters like packet and Ack length, timeslot length, and the time deviation of the two networks. It is worth pointing out that this probability does not give the Packet Reception Ratio (PRR) when two TSCH networks coexist in a single channel. In fact, $\overline{p_c}$ gives the probability with which two networks do not collide when they get close to one another provided that they use the same channel. For the scenario tested in Fig. 5, the chance of collision-free communication is $\overline{p_c} = 63\%$. Fig. 6 visualize this chance ($\overline{p_c}$) calculated for two Ack-enabled networks with various data packet lengths in the range of 22 bytes till 133 bytes, showing that in the chance is up to 82% and 42% in the best and worst case scenarios, respectively. These values increase to 93% and 58% for Ack-disabled networks. This reveals a considerable chance of collision-free communications of two independent networks when they operate in a single frequency channel in a timeslot, showing that it cannot be simply ignored (e.g., [17]).

The chance of overlap in time ($p_c = 1 - \overline{p_c}$) during two co-channel timeslots is calculated using Eqn. 4. If a TSCH network is operating in the Ack-disabled mode, the transmitter does not have information about the success of packet transmission, and the calculated overlap chance gives the packet reception of the link (i.e., from the view point of the receiver). However, when the Ack transmission is enabled, the calculated overlap chance reflects the packet delivery status from the transmitter point of view. It means that if the time overlap happens only during the Ack transmission in a network, the packet is received by the receiver successfully, but the transmitter (of the data packet) does not receive the Ack packet due to collision. Thus, the transmitter counts it as a packet drop while it is a reception from the receiver point of view. Fig. 7 illustrates such a case in a co-channel scenario in which the Ack transmission is enabled in both networks. Note that Ack is not sent in $TSCH_j$ because the data packet of $TSCH_j$ collided with the Ack of $TSCH_i$ and thus the intended

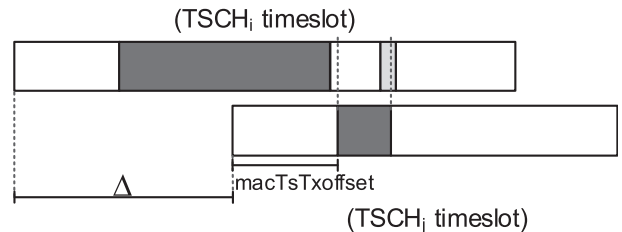


FIGURE 7. An example scenarios with time overlap of co-channel TSCH networks.

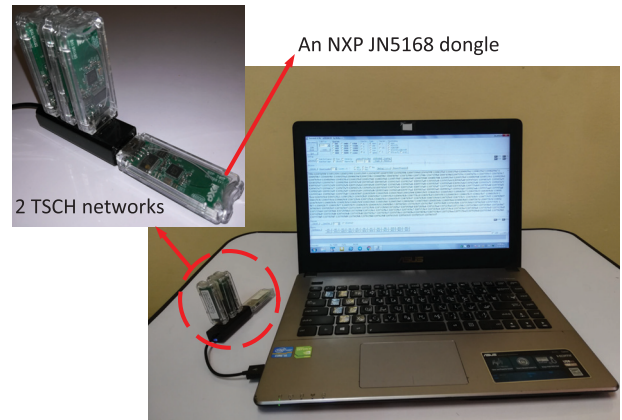


FIGURE 8. Experimental setup used for verification of time overlap analysis.

receiver does not send an Ack back to the transmitter. In the same figure, the transmitter in $TSCH_i$ does not receive the ACK and assumes a packet drop while the data packet has actually received by the intended receiver. As said, Eqn. 4 gives the interference-free chance from the transmitter's point of view. To compute the receiver notion of this chance, we can make the value of the Ack-related indexes in Γ to zero and then compute the convolution. As the last point, note that in the Ack-enabled networks, the transmission of the Ack packet by the intended receiver depends on the successful reception of the data packet. Thus, if the data packet of a network collides with data or Ack packet of another network, the Ack packet will not be transmitted causing vector Γ to be changed. However, this fact does not affect the output of the model since we already count this case as a packet drop for both networks from the transmitter point of view.

C. EXPERIMENTAL MODEL VERIFICATION

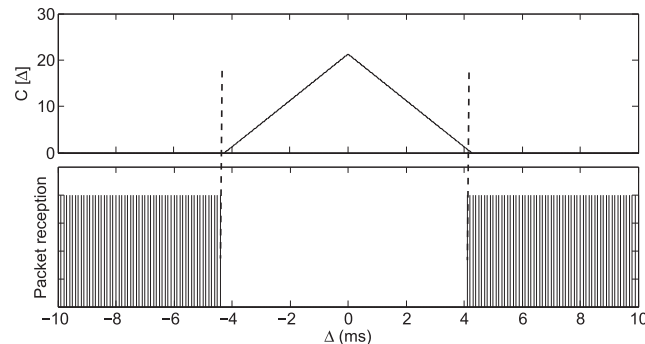
To verify the co-channel collision analysis, we use both practical experiments and simulations. For the experimental setup, we deploy two TSCH networks each consisting of two NXP JN5168 [18] dongles programmed by the TSCH implementation [19] of the Contiki [20] IoT operating System, as depicted in Fig. 8. In each network, one node is constantly sending packets to another in all timeslots. All the nodes are just next to one another, and the experiments are performed in an interference-free environment in which no external wireless communications is expected. Since the nodes are very close to one another and they all use the same transmission power, we do not expect the capture effect

TABLE 1. Cooja simulation results vs. time analysis output for co-channel TSCH networks in Ack-disabled mode.

TSCH 2 \ TSCH 1	$L_{pkt} = 50B$	$L_{pkt} = 90B$	$L_{pkt} = 133B$	
$L_{pkt} = 50B$	89.5	85.3	80.9	Cooja (PRR) model (\bar{p}_c)
	89.3	85	80.4	
$L_{pkt} = 90B$	85.5	81.1	76.7	Cooja (PRR) model (\bar{p}_c)
	85	80.8	76.2	
$L_{pkt} = 133B$	80.9	76.7	72.3	Cooja (PRR) model (\bar{p}_c)
	80.4	76.2	71.7	

TABLE 2. Cooja results vs. analytical model for co-channel networks when Ack transmission is enabled in $TSCH_2$.

TSCH 2 \ TSCH 1	$L_{pkt} = 50B$	$L_{pkt} = 90B$	$L_{pkt} = 133B$	
$L_{pkt} = 50B$	81.9	77.9	73.3	Cooja (PRR) model (\bar{p}_c)
	81.8	77.6	73	
$L_{pkt} = 90B$	73.7	69.3	64.9	Cooja (PRR) model (\bar{p}_c)
	73.3	69	64.4	
$L_{pkt} = 133B$	66.2	61.9	57.5	Cooja (PRR) model (\bar{p}_c)
	65	60.8	56.2	

**FIGURE 9.** The output of the convolution function (overlap ratio) vs. the packet reception status during the experiments.

to cause packet reception during concurrent transmissions. Therefore, any packet reception will mean no time overlap between transmissions in the two networks. Both networks use timeslots of length $T_{ts} = 10\text{ ms}$ and physical layer packets of 133 bytes (i.e., $L_{pkt} = 4256\mu\text{s}$) in the Ack-disabled mode (no Ack packet is transmitted).

In order to test the collisions for different scenarios with respect to the time deviation between the timeslots' boundaries of the two networks ($-10\text{ ms} \leq \Delta \leq 10\text{ ms}$), the beginning of the timeslot of one the TSCH networks is shifted as much as $\delta = 100\mu\text{s}$ after each timeslot. Since we perform the experiment for 200 timeslots, it means that we test the packet reception status while Δ gets its all possible values in its range with a resolution of $100\mu\text{s}$.

Fig. 9 shows the packet reception status as well as the output of the convolution function (Eqn. 3). It is clear from the figure that for Δ values for which the convolution is non-zero, the packets are all dropped and there are no successful packet reception (note that capture effect is not expected to cause reception in the performed experiments). Accordingly, when the convolution gives a zero, all packets are received by the receivers successfully. Note that the used resolution ($\delta = 100\mu\text{s}$) for varying Δ is greater than the symbol duration (i.e., $16\mu\text{s}$) in the standard; it is around

6 symbol durations. Thus, collision in time for a δ period means loosing around 6 symbols (24 bits) assuring the packet to drop.

Considering that controlling time deviations between the timeslot boundaries in different TSCH network is very challenging in real-world experiments, and the need for testing many scenarios, the model verification is extended with several Cooja [21] simulations. It allows us to verify the model in different modes and with various packet lengths. Cooja is the network simulator of the Contiki operating system, which uses the same firmware as the one used in real experiments. Because of that, Cooja simulations provide very accurate results in terms of the exact timing of transmissions in different networks; yet it provides the opportunity to easily set time deviations between the TSCH networks. Since the simulation model of the NXP JN5168 dongles was not available in Cooja, the Z1 platform is used for which the length of timeslots is set to $T_{ts} = 15\text{ ms}$. This allows us to test the analysis in settings different than the default configurations. Both Ack-enabled and Ack-disabled modes are tested. In the Ack-enabled simulation, the Ack packet transmission is only enabled in one of the TSCH networks ($TSCH_2$). After each simulation, the percentage of timeslots with successful packet reception is measured.

Table 1 and Table 2 summarize the Cooja simulation results (PRR) for Ack-disabled and Ack-enabled networks, respectively. Also, the tables present the chance of collision-free communications (\bar{p}_c) given by Eqn. 4. There are several observations from these two tables. First, the results show a very accurate estimation of the collision chance when two TSCH networks are operating in the same frequency channel, since the Cooja results are very close to the output of the model in all the cases. Second, comparing the simulation and model output in Table 1 with those in Table 2 reveals the impact of Ack packet transmission in lowering the chance of collision-free packet transmission. For instance, the case of $L_{pkt} = 133$ bytes, the chance of being collision-free is $\sim 72\%$ in the ack-disabled mode, while it is $\sim 57\%$ when Ack

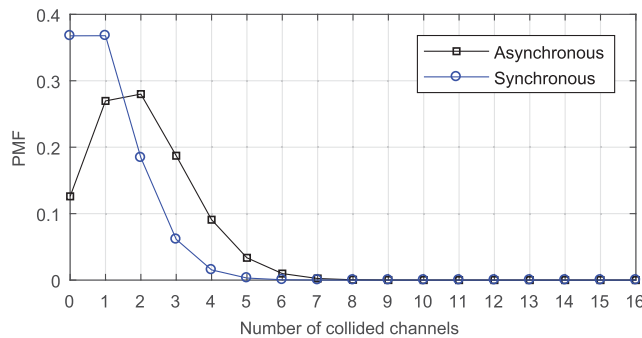


FIGURE 10. PMF of interfered channels for two TSCH networks in sync mode and no-sync mode.

transmission in $TSCH_2$ is enabled. Third, the impact of longer packets in increasing the collision chance is clearly visible.

V. FREQUENCY CHANNEL OVERLAP INVESTIGATION

In the previous section, the chance of collision between two networks operating in the same channel in a timeslot was analyzed. In this section, we present an insight of the chance of frequency channel overlap when several TSCH networks are in the communication range of one another. Based on the IEEE 802.15.4 standard, a TSCH network hops to a different channel from the 16 available channels in the 2.4 GHz based on a preset HSL. Different networks thus have different HSLs meaning that the order of the channels in their HSL may differ. Moreover, even if the HSLs of two TSCH networks are exactly the same, the networks may have no channel overlap since their ASNs are not synchronized or their channel offsets are different. Therefore, the chance of channel overlap depends on the HSL, ASN, and channel offsets of coexisting networks with respect to one another.

To investigate the channel overlap, we first perform Monte Carlo simulations in MATLAB for two networks. Simulations are repeated two million times, each with randomly generated HSLs for the two networks. Two cases of synchronous ($|\Delta| \leq 500\mu s$) and asynchronous scenarios ($|\Delta| > 500\mu s$) are tried. Note that the TSCH standard with its timeslot structure allows the nodes within a single network to deviate from each time-wise up to $500\mu s$, compensated by the guard times at the beginning of the timeslots. However, the chance of synchronous TSCH networks is extremely low since the networks are managed and operated independently.

Fig. 10 presents the Probability Mass function (PMF) for the number of channels with overlap (N_c) between the two networks resulted by the simulations. The PMF of the synchronized networks mode is compliant with a Poisson distribution with $\lambda = 1$. One observation is that the chance of no channel overlap is only 13% in the asynchronous scenario (it is close to 40% for the synchronous one). Also, in both scenarios, the chance of more than 6 channel overlap (out of the 16 used channels in the HSLs) is very low. In the majority of cases when two networks coexist, 1, 2, or 3 channels are affected (synchronous scenario).

To get a better insight of what happens when a number of TSCH networks are close to one another (gathering of

people in the WBAN applications, or several cars behind a traffic light), the Monte Carlo simulations are repeated for different number (N) of coexisting TSCH networks. In this set of simulations, the networks are not synchronized with one another. Fig. 11 gives the histogram of the number of collided channels for various values of N from 2 to 16. Note that the results for maximum 16 number of TSCH networks are shown in this figure to avoid crowded plot, though there is no limit for N in this analysis. However, such a number of networks presented in this figure is a good representative of the number of networks expected to coexist in the application scenarios in mind (e.g., in-vehicle TSCH networks). Moreover, Fig. 11, with this range of N , already shows the trend in the number of affected frequency channels when the number of TSCH networks grows. The most important message of this results is understanding the best and worst cases that may happen when $N \geq 2$ TSCH networks coexist. For example, when $N = 6$, almost the probability of no channel overlap ($N_c = 0$) is almost zero, meaning that even in the best case, there is no hope for unaffected interference from the point of view of each of the six networks. For the same $N = 6$ case, with a probability of only 2%, there are three channels overlapped ($N_c = 3$). On the other hand, the probability of $N_c = 13$ affected channels is almost 2%. The graph shows that for $N = 6$ coexisting TSCH networks, the chance of having 7, 8, or 9 channels overlapped out of the 16 channels are the most possible which happen in around half of the cases (sum of the PMF values for these three number of channels for $N = 6$).

VI. A FULL MULTI-TSCH COEXISTENCE SIMULATOR

When a number of independent TSCH networks are in the communication range of one another, the impact of their communications on one another depends on individual parameters of the coexisting networks (length of timeslots, HSL, packet length, and Ack length), and their time deviations with respect to one another. The previous sections investigated the chance of interference-free coexistence when two networks operate in the same channel in a timeslot, and the chance of channel overlaps for various number of TSCH networks. In this section, a full multi-TSCH coexistence simulator is presented, which receives the parameters of individual networks as its inputs, and simulate their impact on one another resulting the collision rate of each network. Then the simulator is used to give an insight of the performance in the worst/best/average case scenarios of such coexistence.

A. MULTI-TSCH COEXISTENCE SIMULATOR DESIGN

The developed multi-TSCH coexistence simulator is general enough to be able to perform Monte Carlo simulation for any configuration of the involved TSCH networks. For each simulation, the time deviation between the timeslots of different TSCH networks and their HSLs are randomly picked for many iterations to get statistically reliable and stable results. An important aspect of this simulator is its scalability in terms of the number of TSCH networks (N). The main reason is

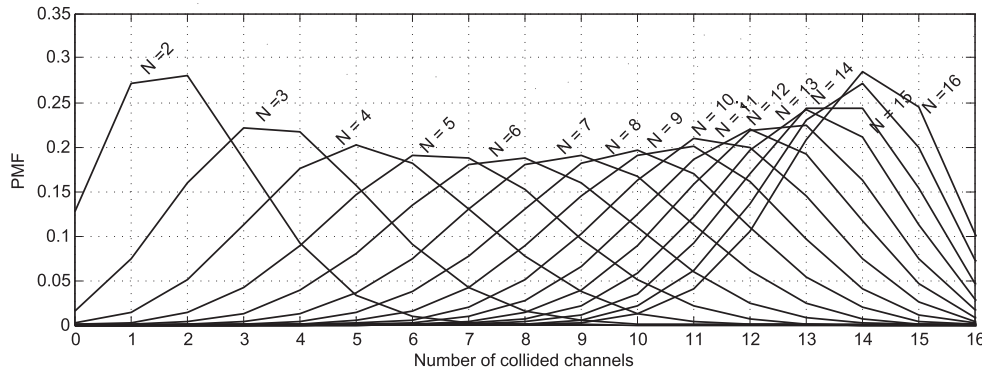


FIGURE 11. PMF of the number of channels with overlap for different number of TSCH networks (N).

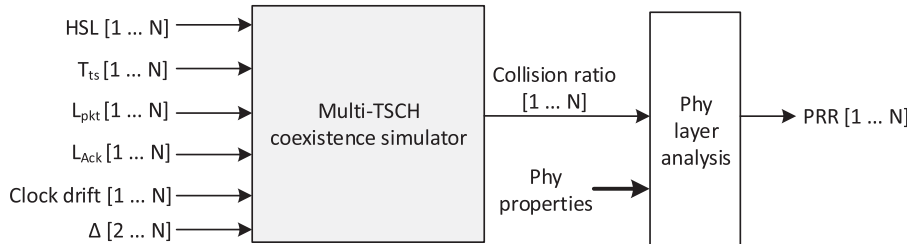


FIGURE 12. The inputs and outputs of the multi-TSCH coexistence simulator for N independent TSCH networks. The simulator results in MAC layer collision probabilities, which can be fed to physical layer models to acquire packet reception ratio.

that this coexistence simulator only determines the used frequency channel and exact time of packet transmission by each TSCH network to find out the chance of overlap in time and frequency between data or Ack packet transmissions in these networks. Thus, despite (event-driven) network simulators such as OMNeT++ or NS3, this coexistence simulator does not care about the content of the packets or details of different layers of the protocol stack to have a very fast execution. This leads to a very scalable simulation of coexistence behavior of any number of TSCH networks in best, worst, and average case scenarios.

In all the discussions in this paper including the multi-TSCH coexistence simulator, there is no assumption or limit regarding the size of each TSCH network. Instead, it is assumed that all timeslots in each slotframe are dedicated for transmission of nodes within each network. The packet transmission is not necessarily done by only one node; any number of nodes can be involved as while as they are in the interference range. It may happen in a big network in which the nodes have low-frequency packet transmissions, or in a small network but with nodes frequently generating data packets. The exact node transmitting in each timeslot is determined by a TSCH scheduler (e.g., [22] and [23]) and is out of the scope of this analysis.

Fig. 12 shows the inputs and outputs of the multi-TSCH coexistence simulator (developed in MATLAB), where N is the number of involved TSCH networks. The timing of the first network is presumed as the time reference. Thus Δ_i ($2 \leq i \leq N$) is the time deviation of $TSCH_i$ with respect to the timing of the first network. Other inputs are the hopping

sequence list (HSL), timeslot length (T_{ts}), data packet length (L_{pkt}), and Ack packet length (L_{Ack}) individually set for each network.

An important aspect considered in this simulator is the clock drift of different networks. The TSCH standard has mechanisms for continuous synchronization of the nodes within a network to eliminate the nodes from getting out of synchronization due to clock drifts. Although the synchronization mechanisms keep the nodes' timeslot boundaries aligned within a TSCH network, the relative time differences between independent TSCH networks may change over time. This can dynamically change the coexistence scenario of these networks while they are operating in proximity of one another. The developed simulator gets the clock drift of each network as an input, and takes it into account in estimating the collision ratio between the involved TSCH networks.

Like in the time-domain analysis, a vector (Γ_i) with a resolution of δ is made for each network $TSCH_i$. Each element of these vectors is zero when there is no transmission in that moment according to the exact timing of the protocol standard and the given parameters. When a data or Ack packet is being sent in a network, the corresponding elements get the channel number as their value. Thus the overlaps in both time and frequency channel between the networks can be extracted. If the data or Ack packet transmission of a network overlaps in time and frequency with at least one other network, it is counted as a collision which can lead to a packet drop depending on the specifications of the collided signals in the physical layer. Note that in the Ack-enabled networks, the Ack transmission in a timeslot depends on

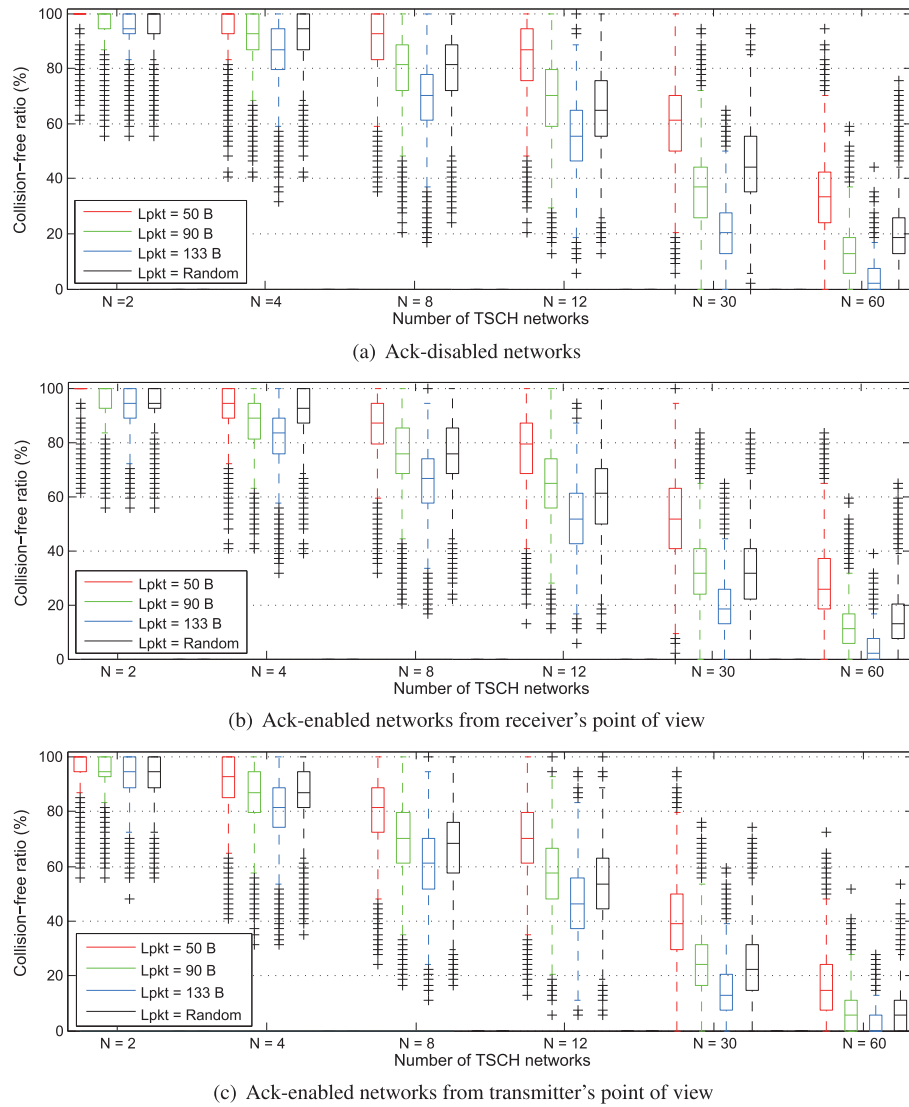


FIGURE 13. The chance of interference-free coexistence of N independent TSCH networks. Clock drift is disabled in this set of simulations.

the collision-free transmission of its data packet in the same timeslot. Therefore, the vectors (Γ_i) are made during the execution of the simulations for each timeslot. This simulator is publicly available to the community through the web site <http://www.es.ele.tue.nl/nes/>.

B. SIMULATION RESULTS: COEXISTENCE ANALYSIS

To get a better insight about the performance of TSCH networks in the vicinity of one another, a number of setups with different parameters are tested using the developed simulator. For each setup, the simulations are repeated 500000 times, each with randomly picked time deviation for each network ($0 \leq \Delta_i \leq T_{ts}$), and randomly shuffled frequency channels to make the hopping sequence list for each network (HSL_i). In all cases, it is assumed that $|HSL_i| = 16$ and $T_{ts}^i = 10ms$ for all networks. The clock drift is disabled for this set of simulations to be able to analyze the coexistence behavior at an instance of time. In the later set of simulations, the impact of clock drifts is investigated. In this

set of simulations, we investigate the impact of inter-TSCH interferences for different number of coexisting networks ($N = 2, 4, 8, 12, 30, 60$) and packet lengths ($L_{pkt} = 50, 90, 133, random$ (50 – 133) bytes). The lower values of N are to represent the typical number of networks in application scenarios in mind (in-vehicle networks or WBANs). The two values of $N = 30$ and $N = 60$ are tested to firstly understand the coexistence behavior in rare scenarios with very dense TSCH networks' coexistence, and secondly to examine the scalability of the developed simulator. Fig. 13 shows the results of the simulations for different network setups.

Fig. 13(a) presents the estimated chance of collision-free packet transmission resulted out of the simulations for Ack-disabled networks. The results show the impact of packet lengths on inter-TSCH interference. For instance, for $N = 2$, the difference between average collision-free ratio when $L_{pkt} = 50$ bytes and $L_{pkt} = 133$ is around 5%. This difference increases to 33% for $N = 12$. This may suggest that using

shorter packets can considerably improve the performance of the TSCH-based IoT networks when they are expected to coexist with other independent TSCH networks. Also, the boxplots clearly reveal the effect of N on both the average case and the worst case scenarios. For the case of $N = 12$ and $L_{pkt} = 133$, there are samples that end up with a very low collision-free ratio as low as just 5% while, in exactly the same case, we have samples with almost no inter-TSCH interference resulting in a PRR very close to 100%. It means that although the number of coexisting networks are not under the control, it may be possible to alter the design and adaptively configure the individual networks in such a way so that we decrease the chance of trapping in the worst case scenario. This is important because it can lead us to solutions for reducing the impact of coexisting TSCH network on one another.

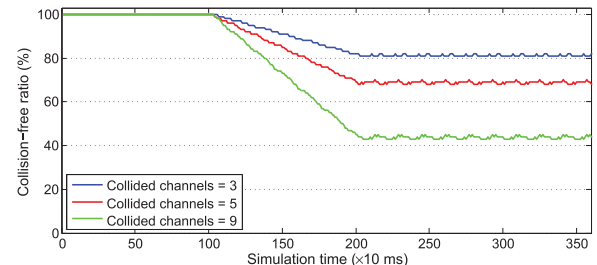
The two cases with $N = 30$ and $N = 60$ number of TSCH networks have resulted in very severe degradation in the collision-free ratio. For $N = 60$, in very rare cases, the collision-free ratio of the Ack-disabled networks can be up to 40%, while the majority of cases have very low collision-free ratio (less than 10%), especially for longer packets. Such results clearly show that TSCH networks are not reliable when a rather high number of these networks coexist.

Fig. 13(b) and Fig. 13(c) show the results of the simulations for Ack-enabled networks from receiver and transmitter points of view, respectively. The size of the Ack packet for all networks is set to $L_{Ack} = 11$ bytes (Imm-Ack type). First, comparing these results with the results of Ack-disabled mode (Fig. 13(a)), the effect of Ack packet transmissions on degrading the performance of coexisting networks is understood. For all N and L_{pkt} values, the collision-free ratio of Ack-enabled mode is clearly lower than those in the Ack-disabled mode. For example, in $N = 12$ and $L_{pkt} = 133$, the collision-free ratio difference between Fig. 13(a) and Fig. 13(b) is close to 4%. In these simulations, the smallest standard Ack length is used. Definitely, larger Ack packets will lead to increased interference chance.

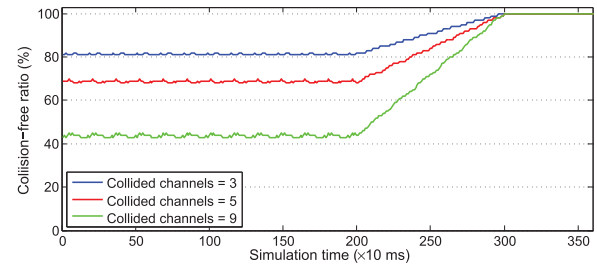
When Ack transmission is enabled in a network, the transmitter of a link considers a packet as successfully delivered to the receiver when it receives the corresponding Ack. Thus, if the Ack packet collides with the data packet or Ack of another network, the transmitter assumes a data packet drop. The differences between the results in Fig. 13(b) and Fig. 13(c) is because of this difference in the view of the receiver and transmitter.

C. IMPACT OF CLOCK DRIFT

To observe and investigate the impact of clock drift on the coexistence behavior of TSCH networks, we run a number of simulations with clock drifts enabled. In the first set of simulations, the aim is to observe the changes that clock drift may make over time on the collision ratio between two coexisting TSCH networks. The packet length is set to 40 bytes and the networks are in the Ack-disabled mode. To be able to catch



(a) Results of simulations with clock drifts for Scenario 1



(b) Results of simulations with clock drifts for Scenario 2

FIGURE 14. The chance of collision-free coexistence over time for two networks with clock drifts. The window length of the moving average is 100.

such an impact, special initial cases are set in such a way that cumulative drift changes the collision status of the networks within the time window under observation. Two scenarios are examined. In Scenario1, the two networks have initial time deviation $\Delta = 1340\mu s$ with respect to each other. This initial time deviation does not lead to any time overlap, but it is very close. We consider the typical clock drift of $\pm 30 ppm$ [24], which corresponds to a mutual drift of maximum $0.6\mu s$ per each timeslot of $T_{ts} = 10 ms$. Fig. 14(a) shows the collision-free ratio over time averaged using a sliding window of 100 instances. The HSLs of the two networks are set in such a way to cause 3, 5, or 9 overlapped channels out of all 16 used frequency channels. The figure shows that after 100 timeslots (corresponding to a cumulative drift of $60\mu s$), transmissions of the two networks start overlapping in time changing the collision-free ratio from 100% to lower values depending on the number of collided channels. This special situation is an instance of cases in which the clock drift can deteriorate the performance of coexisting TSCH networks.

In Scenario2, the aim is to catch an opposite situation in which the two networks have time overlap at the beginning of the simulations and clock drift takes the networks out of this state after a while. The only difference with Scenario1 is that the initial time deviation between the two networks is $\Delta = 1160\mu s$ in this scenario. Fig. 14(b) shows the average collision over time. After 200 timeslots (i.e., cumulative drift of $120\mu s$), the packet transmissions of the networks do not overlap in time anymore and thus no collision is detected.

To investigate the impact of clock drift on the overall coexistence behavior, we run a set of Monte Carlo simulations for two TSCH networks with the same setting as for the simulations presented in Fig. 13(a), but with clock drift enabled. This enables a direct comparison with the

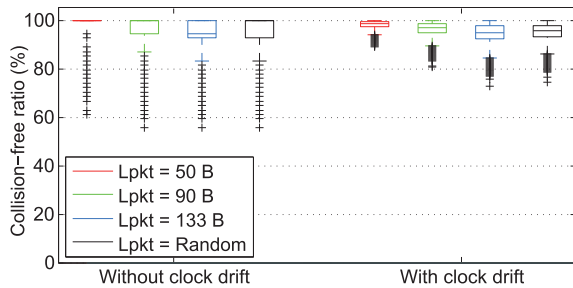


FIGURE 15. The collision-free ratio of two coexisting TSCH networks with clock drift enabled and disabled.

clock drift disabled simulations to understand how clock drift affects the coexistence behavior. Fig. 15 shows the distribution of collision-free ratio resulted from these simulations. The first observation is that clock drift slightly decreases the collision-free ratio for average cases, but the difference is very marginal. The second and more important observation is that clock drift has improved the performance of the worst case scenarios. This is because of cases like what observed in Fig. 14(b). The networks that are overlapping in time and frequency for a major ratio of their transmissions may get a chance to get out of such hassle, and start deviating from each other over time due to cumulative clock drift. This is an important finding since it shows that clock drift between various coexisting TSCH networks can eliminate the networks from trapping in the worst case coexisting scenario for a very long time. The third observation is that the clock drift has not changed the best cases (still 100% collision-free ratio for some simulations). This is because there are some HSL combinations that never make any channel overlap and thus the time deviation does not play any role for those cases.

D. DISCUSSION: PHYSICAL LAYER EFFECTS

The analysis presented in this paper tries to give an insight about the chance of inter-TSCH interferences and their severity in the MAC layer, providing the ratio of packet transmissions in each network that have overlap in time and frequency channel with transmissions of the other TSCH networks. Note that there may be cases that two concurrent transmissions are successful depending on their signal power difference at the location of the intended receivers, known as the capture effect. Investigations presented in [25] show that the impact of capture effect is not negligible for TSCH networks. Among others, the difference in signal strength may be because of using different transmission powers by individual nodes in various networks, difference in the distance between the transmitter and the intended receiver, and the characteristics of the environment (path loss and multi-path fading effects) between the transmitter-receiver pairs. Therefore, the packet reception ratio may be slightly higher than the MAC layer collision-free transmission ratio investigated in this work.

As shown in Fig. 12, the output of the multi-TSCH coexistence simulator, the MAC layer collision ratio, is fed to a physical layer model to include the capture effect and any other physical layer impact, and finally estimate the packet

reception ratio. The physical layer model then needs to get physical layer specifications such as the transmission power of nodes, radio channel characteristics, and distances between various nodes in the TSCH networks.

VII. CONCLUSION

This paper investigates the impact of coexisting independent asynchronous TSCH networks on one another when they are in the communication (interference) range of one another. The goal is to get an insight about the performance of a TSCH network when it operates in the vicinity of other TSCH networks, like in the intra-vehicle network applications. First, assuming that the frequency channels of two networks are the same in a timeslot, the chance of intra-TSCH interference in time is analyzed and modeled. It is shown that there may be still a high chance of interference-free communications for co-channel TSCH networks. Then the chance of being co-channel in some frequency channels when a number of TSCH networks are close to one another is analyzed using Monte Carlo simulations. A full multi-TSCH coexistence simulator is developed by which a detailed insight about the performance of coexisting TSCH networks in worst, best, and average case scenarios is made available. The developed simulator is publicly available to the community.

As a followup research, the finding of this paper can be used to develop proper mechanisms that can adaptively tune the parameters of the TSCH networks that expect to coexist with other TSCH networks in some periods of time. The aim is then to avoid trapping in the worst case coexistence scenarios. Such run-time adaptive mechanisms can be very effective to decrease the chance of disconnections.

REFERENCES

- [1] IEEE 802.15.4-2015 Standard for Low-Rate Wireless Networks, Standard IEEE Std 802.15.4-2015, Apr. 2016.
- [2] R. Tavakoli, M. Nabi, T. Basten, and K. Goossens, “Topology management and TSCH scheduling for low-latency convergecast in in-vehicle WSNs,” *IEEE Trans. Ind. Informat.*, vol. 15, no. 2, pp. 1082–1093, 2019.
- [3] F. Veisi, M. Nabi, and H. Saidi, “An empirical study of the performance of IEEE 802.15.4e TSCH for wireless body area networks,” in *Proc. IEEE Wireless Commun. Netw. Conf. (WCNC)*, Apr. 2019, pp. 1–6.
- [4] L. Angrisani, M. Bertocco, D. Fortin, and A. Sona, “Experimental study of coexistence issues between IEEE 802.11b and IEEE 802.15.4 wireless networks,” *IEEE Trans. Instrum. Meas.*, vol. 57, no. 8, pp. 1514–1523, Aug. 2008.
- [5] W. Yuan, X. Wang, and J.-P. M. Linnartz, “A coexistence model of IEEE 802.15.4 and IEEE 802.11 B/G,” in *14th IEEE Symp. Commun. Veh. Technol.*, Benelux, U.K., 2007, pp. 1–5.
- [6] R. Natarajan, P. Zand, and M. Nabi, “Analysis of coexistence between IEEE 802.15.4, BLE and IEEE 802.11 in the 2.4 GHz ISM band,” in *Proc. 42nd Annu. Conf. IEEE Ind. Electron. Soc.*, Oct. 2016, pp. 6025–6032.
- [7] *Bluetooth Core Specification, V5.0*, Standard, Bluetooth SIG, Dec. 2016, pp. 1–2822.
- [8] M. Balodhi, V. Bijalwan, and B. Negi, “Zigbee and IEEE 802.11b (WLAN) coexistence in ubiquitous network environment,” *Coexistence*, vol. 802, p. 4, Oct. 2014.
- [9] M. Gursu, M. Vilgelm, S. Zoppi, and W. Kellerer, “Reliable co-existence of 802.15.4e TSCH-based WSN and Wi-Fi in an aircraft cabin,” in *Proc. IEEE Int. Conf. Commun. Workshops (ICC)*, May 2016, pp. 663–668.
- [10] J. Kim, W. Jeon, K.-J. Park, and J. P. Choi, “Coexistence of full-duplex-based IEEE 802.15.4 and IEEE 802.11,” *IEEE Trans. Ind. Informat.*, vol. 14, no. 12, pp. 5389–5399, Dec. 2018.

- [11] S. S. Wagh, A. More, and P. R. Kharote, "Performance evaluation of IEEE 802.15.4 protocol under coexistence of WiFi 802.11b," *Procedia Comput. Sci.*, vol. 57, pp. 745–751, 2015.
- [12] J. Bauwens, B. Jooris, P. Ruckebusch, D. Garlisi, J. Szurley, M. Moonen, S. Giannoulis, I. Moerman, and E. De Poorter, "Coexistence between IEEE 802.15.4 and IEEE 802.11 through cross-technology signaling," in *Proc. IEEE Conf. Comput. Commun. Workshops*, May 2017, pp. 529–534.
- [13] M. Chwalisz and A. Wolisz, "Towards efficient coexistence of IEEE 802.15.4e TSCH and IEEE 802.11," in *Proc. IEEE/IFIP Netw. Operations Manage. Symp.*, Apr. 2018, pp. 1–7.
- [14] O. Carhacioglu, P. Zand, and M. Nabi, "Cooperative coexistence of BLE and time slotted channel hopping networks," in *Proc. IEEE 29th Annu. Int. Symp. Pers., Indoor Mobile Radio Commun. (PIMRC)*, Sep. 2018, pp. 1–7.
- [15] C. Ma, J. He, H.-H. Chen, and Z. Tang, "Uncoordinated coexisting IEEE 802.15.4 networks for machine to machine communications," *Peer Netw. Appl.*, vol. 7, no. 3, pp. 274–284, Sep. 2014.
- [16] T. van der Lee, S. Raza, G. Exarchakos, and M. Gunes, "Towards co-located TSCH networks: An inter-network interference perspective," in *Proc. IEEE Global Commun. Conf. (GLOBECOM)*, Dec. 2018, pp. 1–7.
- [17] S. Ben Yaala, F. Théoleyre, and R. Bouallegue, "Cooperative resynchronization to improve the reliability of colocated IEEE 802.15.4 -TSCH networks in dense deployments," *Ad Hoc Netw.*, vol. 64, pp. 112–126, Sep. 2017.
- [18] NXP Semiconductors. (Oct. 2018).JN516x IEEE802.15.4 Wireless Microcontroller. [Online]. Available: <http://www.nxp.com/docs/en/data-sheet/JN516X.pdf>
- [19] S. Duquennoy, A. Elsts, B. A. Nahas, and G. Oikonomo, "TSCH and 6TiSCH for contiki: Challenges, design and evaluation," in *Proc. 13th Int. Conf. Distrib. Comput. Sensor Syst. (DCOSS)*, Jun. 2017, pp. 1–7.
- [20] A. Dunkels, B. Gronvall, and T. Voigt, "Contiki—A lightweight and flexible operating system for tiny networked sensors," in *Proc. 29th Annu. IEEE Int. Conf. Local Comput. Netw.*, 2004, pp. 1–7.
- [21] F. Osterlind, A. Dunkels, J. Eriksson, N. Finne, and T. Voigt, "Cross-level sensor network simulation with COOJA," in *Proc. 31st IEEE Conf. Local Comput. Netw.*, Nov. 2006, pp. 641–648.
- [22] R. Soua, P. Minet, and E. Livolant, "Wave: A distributed scheduling algorithm for convergecast in IEEE 802.15.4e TSCH networks," *Trans. Emerg. Telecommun. Technol.*, vol. 27, no. 4, pp. 557–575, Apr. 2016.
- [23] N. Accettura, M. R. Palattella, G. Boggia, L. A. Grieco, and M. Dohler, "Decentralized traffic aware scheduling for multi-hop low power lossy networks in the Internet of Things," in *Proc. IEEE 14th Int. Symp.*, Jun. 2013, pp. 1–6.
- [24] T. Chang, T. Watteyne, K. Pister, and Q. Wang, "Adaptive synchronization in multi-hop TSCH networks," *Comput. Netw.*, vol. 76, pp. 165–176, Jan. 2015.
- [25] D. D. Guglielmo, B. A. Nahas, S. Duquennoy, T. Voigt, and G. Anastasi, "Analysis and experimental evaluation of IEEE 802.15.4e TSCH CSMA-CA algorithm," *IEEE Trans. Veh. Technol.*, vol. 66, no. 2, pp. 1573–1588, 2016.



FARZAD VEISI received the M.Sc. degree in telecommunications engineering from the Isfahan University of Technology, Isfahan, Iran, in 2019. He is currently working as a Researcher with the Department of Electrical and Computer Engineering, Isfahan University of Technology. His research interests include wireless sensor networks, wireless body area networks, and networked embedded systems.



MAJID NABI (Member, IEEE) received the B.Sc. degree in computer engineering from the Isfahan University of Technology, the M.Sc. degree in computer engineering from Tehran University, and the Ph.D. degree in electrical and computer engineering from the Eindhoven University of Technology (TU/e), Eindhoven, The Netherlands, in 2013. He is currently an Assistant Professor with the Department of Electrical Engineering, TU/e, and the Isfahan University of Technology. His research interests include efficient and reliable networked embedded systems, low-power wireless sensor networks, and the Internet of Things.



HOSSEIN SAIDI received the B.S. and M.S. degrees in electrical engineering from the Isfahan University of Technology (IUT), Isfahan, Iran, in 1986 and 1989, respectively, and the D.Sc. degree in electrical engineering from Washington University in St. Louis, USA, in 1994. Since 1995, he has been with the Department of Electrical and Computer Engineering, IUT, where he is currently a Full Professor. He holds four USA patents and one international patent and has published more than 100 scientific articles. His research interests include high-speed switches and routers, communication networks, QoS in networks, security, queueing systems, and information theory. He was a recipient of several awards, including the 2006 ASPA Award (The 1st Asian Science Park Association Leaders Award) and the Certificate Award at 1st National Festival of Information and Communication Technology (ICT 2011) as the CEO of SarvNet Telecommunication Inc.

• • •